Electronic Supplementary Material (ESI) for Journal of Materials Chemistry C.

Electronic Supplementary Information for

Novel Up-Conversion Photoluminescent Materials:

Noncoherent Excitation by Near-Infrared Sunlight

Cheng Chen, Ting Cao, Lijian Liu*
Key Laboratory of Biomedical Polymers, Ministry of Education, College of Chemistry and Molecular Sciences, Wuhan University, Wuhan, 430072, China.
Correspondence to: Lijian Liu (E-mail: liulj@whu.edu.cn)

Materials. Ethyl diazoacetate (EDA) was prepared based on literature methods.[1, 2] 2-Hydroxyethyl acrylate (product of Japan) and poly(ethylene glycol) methyl ether acrylate (average M_n of 480, product of Japan) were purchased from Sigma-Aldrich Co., Ltd. Acrylyl chloride (98%) was purchased from Energy Chemical Industry Co., Ltd. N-isopropylacrylamide (99%), styrene (99.5%) and ethyl acrylate (99.5%) were purchased from Acros Organics. Azodiisobutyronitrile (AIBN) and benzoyl peroxide (BPO) were purchased from Alfa Aesar and recrystallized from ethanol before use. Other reagents were purchased from Sinopharm Chemical Reagent Co., Ltd.

Instruments. ^{1}H-NMR and ^{13}C-NMR spectra were recorded using a Bruker 400M spectrometer with $CDCl_3$ as the solvent and TMS as the internal standard. The number-average molecular weights (M_n) and polydispersity indices (PDI, M_w/M_n) of the oligomer samples were determined using gel permeation chromatography (GPC) calibrated with polystyrene standards, and tetrahydrofuran (THF) was used as the eluent (1.0 mL min^{-1}) at 30 °C (both the columns and detector). Fourier transform infrared (FT-IR) spectra were recorded using a Thermo iS10 spectrometer. Elemental analysis data were collected using a Vario EL instrument. Matrix-assisted laser desorption ionization time-of-flight mass (MALDI-TOF-MS) spectra were obtained using a Bruker Biflex III mass spectrometer equipped with a 337-nm nitrogen laser. The glass-transition temperature data were collected using a Q20 instrument (TA Instruments) with nitrogen as the protecting gas (50 mL min^{-1}). Fluorescence emission and excitation spectra were recorded on an RF-5301PC (Shimadzu) fluorescence spectrophotometer with a 150 W Xe lamp as the light source, and the slit width was set at 5.0 for both monochromators. A 300 W Xe lamp (PLS-SXE 300, Beijing Perfectlight Co. Ltd) was used as simulated sunlight source and a supfire UV03-365 flashlight used as single 365 nm light source. The optical induction current value of the incident light was measured by a solar panel connected to a multimeter, and the power of the incident light was measured by a UVA light meter (Model UVA-365). Ultraviolet-visible (UV-vis) spectra were obtained using a UV-3600 (Shimadzu) spectrometer. Confocal fluorescence micrographs were recorded using confocal laser scanning microscopy (CLSM; Nikon C1-si, Japan, BD Laser) at 405 nm, 700 nm and 405 + 700 nm.

Preparation of 3-carbethoxy-5-acrylatecarbethoxy-2-pyrazoline (CACP). In a double-necked flask (250 mL) fitted with a stirrer and thermometer, we added 2-hydroxyethyl acrylate (1.1612 g, 0.01 mol), EDA (1.1440 g, 0.01 mol), and ethyl acetate (20 mL) and stirred the mixture for 24 h at 30 °C. Subsequently, the crude product was purified by silica gel chromatography to obtain 3-carbethoxy-5-hydroxymethylcarbmethoxy-2-pyrazoline (CHCP, 2.1621 g, 94%).In a three-necked flask (250 mL) fitted with a stirrer, dropping funnel, and thermometer, a solution of CHCP (1.8442 g, 8mmol) in chloroform (100 mL) was added. A solution of triethylamine, prepared from triethylamine (1.2 mL, 8.7 mmol) and chloroform (10 mL), was added with stirring at 25 °C for 10 minutes. After the addition was completed, the mixture was stirred in an ice bath for an additional 30 minutes, and a solution of acryloyl chloride that was prepared from acryloyl chloride (0.65 mL, 8 mmol) and chloroform (10 mL) was added dropwise with stirring so that the reaction

mixture remained within the temperature range 0-5 °C (Approximately 30 minutes was required for the addition). After the addition was completed, the mixture was stirred for 2 h and then purified by silica gel chromatography to obtain CACP (0.9315 g, 41%).

General synthetic procedure for the polymerization of CACP. A 50-mL three-necked round-bottomed flask was equipped with a Teflon-coated magnetic stir bar, a reflux condenser, which was connected to a safety bottle padded with silicone oil to insulate the air, a 10-mL pressure-equalizing dropping funnel containing AIBN (32.8 mg, 0.2 mmol) and 5 mL of toluene, and the flask was sealed with a glass plug and had a tube fitted with a dry N_2 gas inlet. The flask was flushed with N_2 and charged with CACP (0.284 g, 1 mmol) and 10 mL of toluene. After 30 minutes of N_2 protection, the AIBN solution was added dropwise, and the mixture was stirred and heated to 70 °C for 24 h. The obtained product was dissolved in toluene and precipitated by ethyl ether at least 3 times. Finally, the product was dried under vacuum for 24 h. Other experiments were performed in the same manner.

Cell imaging. Human cervical carcinoma (HeLa) cells were purchased from the China Center for Type Culture Collection and incubated in a complete medium (Dulbecco's modified Eagle's medium (DMEM) supplemented with 10% fetal bovine serum (FBS)) with 1% antibiotics and 5% CO_2 at 37 °C. The cells were seeded in a 6-well plate at a density of 2×10^5 cells per well and cultured in 1 mL of the complete medium for 24 h. Then, a solution of the oligomer (OCACP, run 1, 50 μg) was dissolved in DMEM (1 mL), and 10% FBS, 1% antibiotics and 5% dimethyl sulfoxide were added. The solution was incubated for another 4 h at 37 °C. The cells were then washed with PBS (1 mL) after the medium was removed, and CLSM was performed at 405 nm, 700 nm and 405 + 700 nm.

Design of OCACP. Compared with 3,5-dicarbethoxy-2-pyrazoline, 3-carbethoxy-2-pyrazoline-grafted polyvinyl alcohol (CEP-g-PVA) shows weaker Rayleigh scattering and a higher quantum yield, as previously reported[3] but for a grafting ratio of 12.12%, and the fluorescence enhancement was weak. Thus, 3,5-dicarbethoxy-2-pyrazoline was reacted with acryloyl chloride to obtain 1-propenone-3,5-dicarbethoxy-2-pyrazoline (PDP, Scheme S1 and Figure S1). After free radical polymerization, the oligomer (OPDP, Figure S2) of PDP with a 100% grafting ratio showed an enhancement in fluorescence (Figure S3), but the fluorescence intensities of the polymer and monomer were extremely weak (the quantum yield of PDP and OPDP are $1.43*10^{-4}$ and $3.56*10^{-4}$). This indicated that the reactive hydrogen on the pyrazoline ring was replaced by a propenone group, which resulted in the disruption of the electronic radiation transition from a conjugated N=C-C=O group to a delocalized N-N=C system.[4] Thus, we synthesized 3-carbethoxy-5-hydroxymethylcarbmethoxy-2-pyrazoline (CEHMP) with two reactive hydrogens and reacted it with acryloyl chloride. After the purification process, the reactive hydrogen on the pyrazoline ring was retained, and the other reactive hydrogen was replaced by a propenone group. The product showed good fluorescence properties. In addition, the product could be polymerized by a free-radical initiator, and the

excellent fluorescence behavior of the obtained polymer was observed.

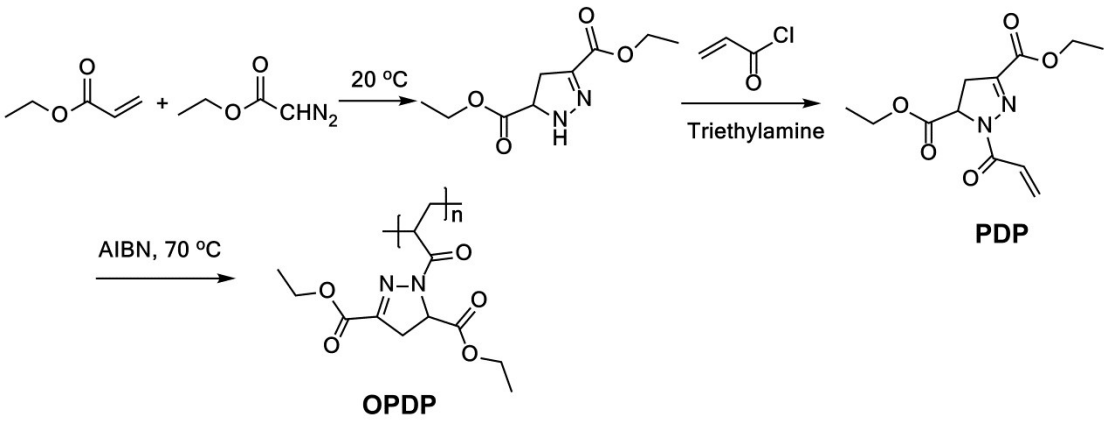

Scheme S1 The synthesis process of PDP and OPDP.

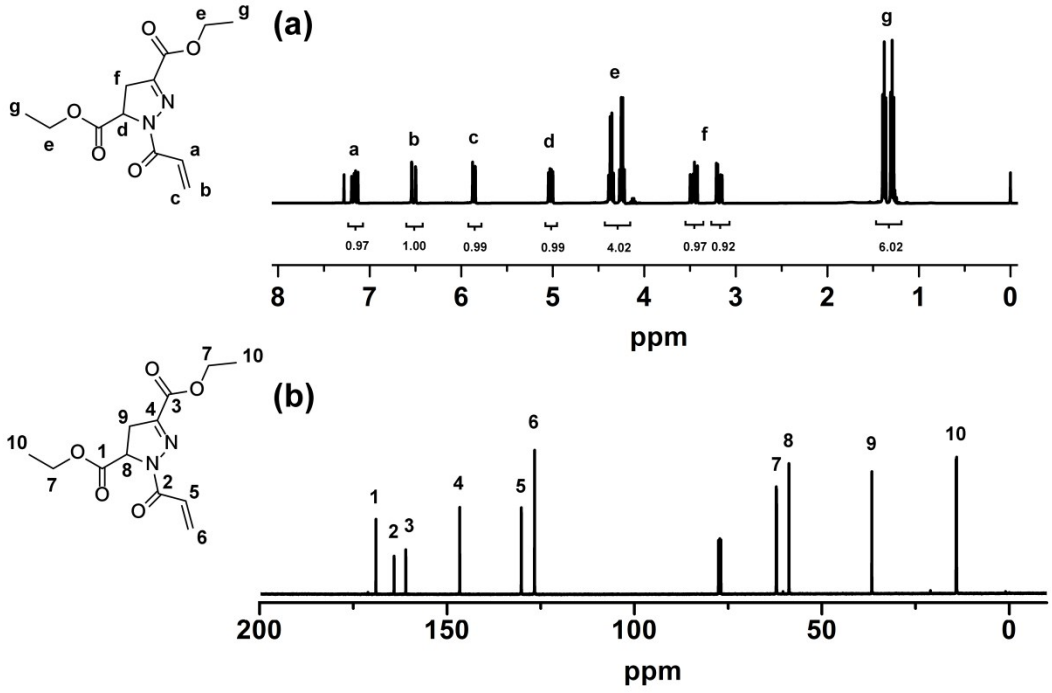

Figure S1 The ^{1}H NMR (a) and ^{13}C NMR (b) spectrum of PDP.

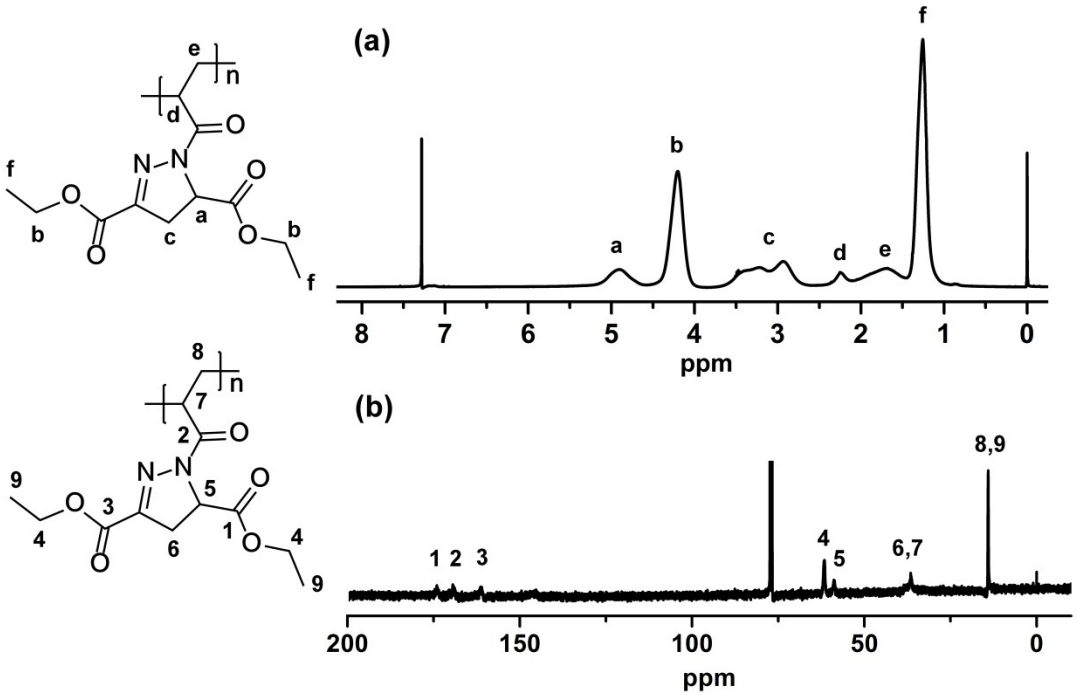

Figure S2 The ^{1}H NMR (a) and ^{13}C NMR (b) spectrum of OPDP.

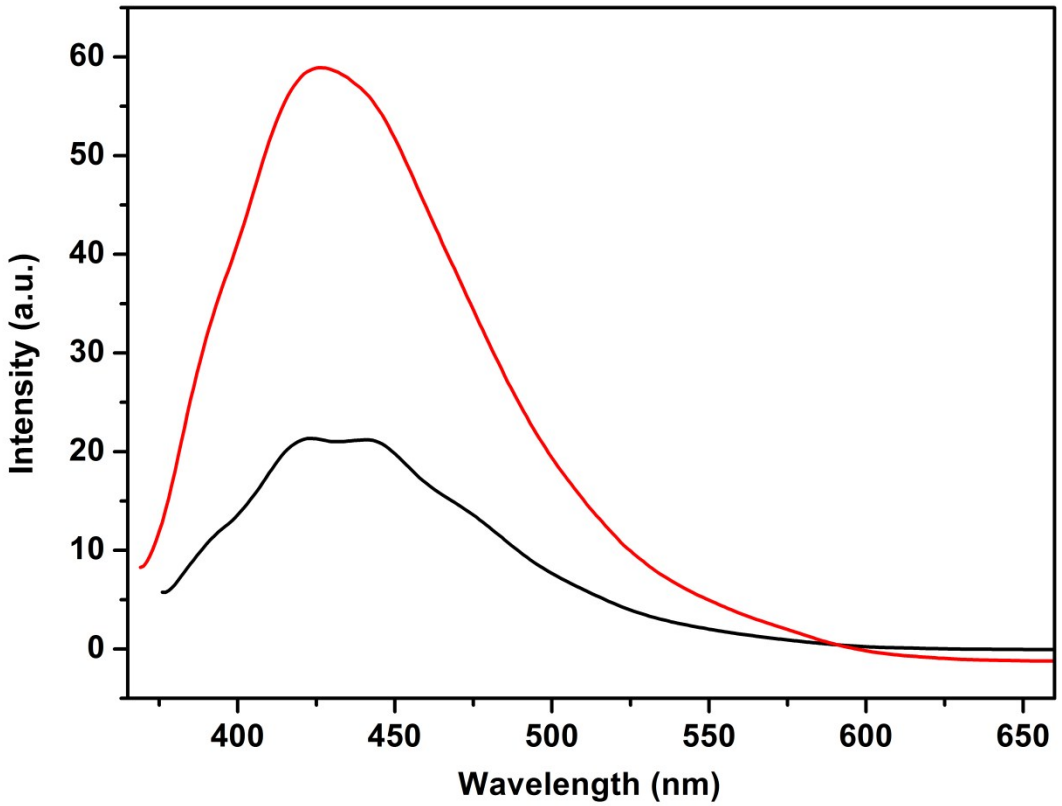

Figure S3 The fluorescence emission spectrum of 1 mg mL^{-1} of PDP (black line) and OPDP (red line) in chloroform with the slit width set at 5.0 for both monochromators.

Characterization of CACP. CEHMP was synthesized by a 1,3-dipolar cycloaddition of EDA with 2-hydroxyethyl acrylate (Scheme S2 and Figure S4). After the addition of deuteroxide, the signals at δ 7.11 and 7.29 disappeared (Figure S4), which indicated that the two reactive hydrogens exchanged with deuterium. Subsequently, CEHMP was reacted with acryloyl chloride to obtain two main products. Then, deuteroxide was added, and in the two NMR spectra, one peak disappeared (Figure S5). To further characterize the two products, we compared the NMR spectra of PDP with those of the two products (Figure S6). Then, CACP was clearly characterized. As shown in Figure S7a, the signals near δ 6.76 ppm are assigned to -NH-, and the signals near δ 6.44-5.87 ppm are attributed to -CH=CH_2. The signals at δ 4.52-4.39 ppm are ascribed to -$COOCH_2CH_2COO$- and -CH<, respectively. The signals near δ 4.34-4.20 ppm are attributed to the methylene groups (OCH_2) that are connected to the methyl group. The signals near δ 3.37-3.15 ppm are ascribed to the methylene (CH_2) group in the pyrazoline ring, and the signals at δ 1.32 ppm are assigned to the methyl group. The ^{13}C NMR spectrum of CACP is shown in Figure S7b. The peaks near δ 13.24 ppm indicate the methyl group (CH_3), and the peaks near δ 33.48 ppm are attributed to the methylene (CH_2) group of the pyrazoline ring. The peaks near δ 62.58-60.33 ppm are ascribed to the methylene group (OCH_2) and methyne group (CH) that are connected to the nitrogen atom. The peaks at δ 126.75 and 130.94 indicate the double bond. The peaks at δ 141.26 ppm are attributed to the C=N group, and the peaks at δ 170.30, 164.57 and 160.75 ppm are assigned to the carbonyl group.

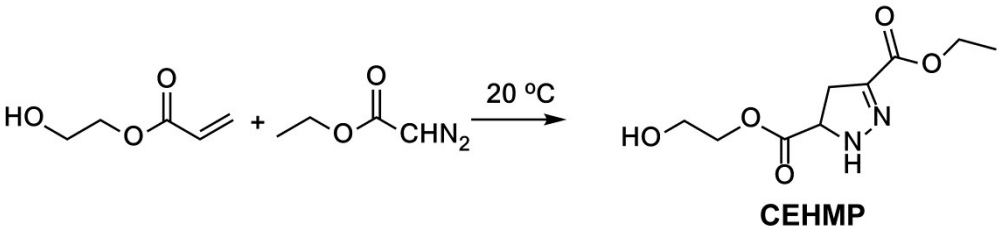

Scheme S2 The synthesis process of CEHMP.

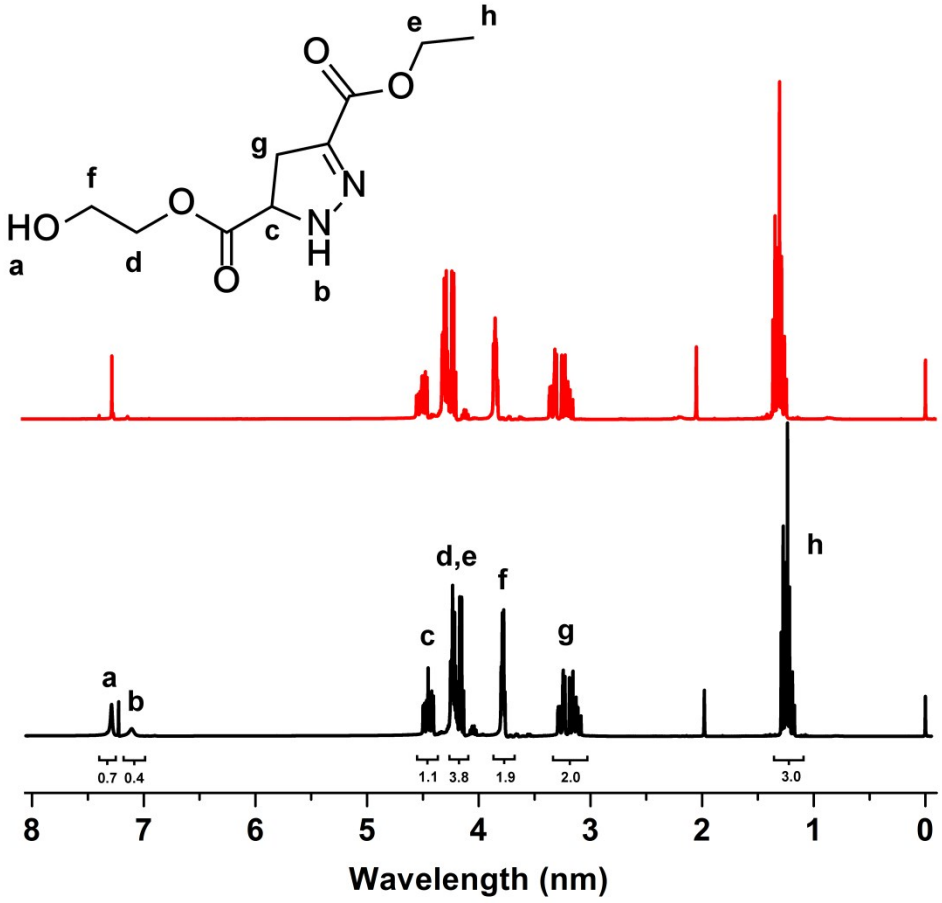

Figure S4 The ^{1}H NMR spectrum of CEHMP (black line) and added deuteroxide (red line).

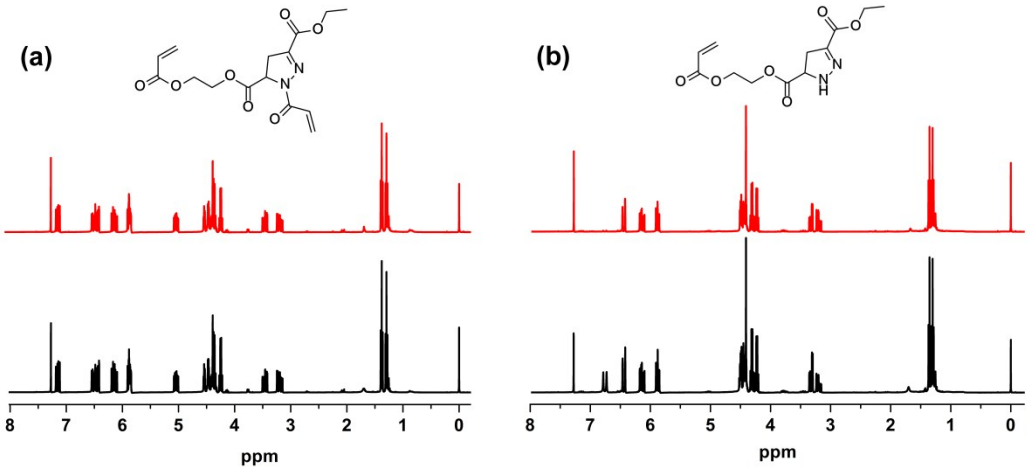

Figure S5 (a) The ^{1}H NMR spectrum of 1-propenone-3-carbethoxy-5-acrylatecarbethoxy-2-pyrazoline (PCAP, black line) and added deuteroxide (red line). (b) The ^{1}H NMR spectrum of CACP (black line) and added deuteroxide (red line).

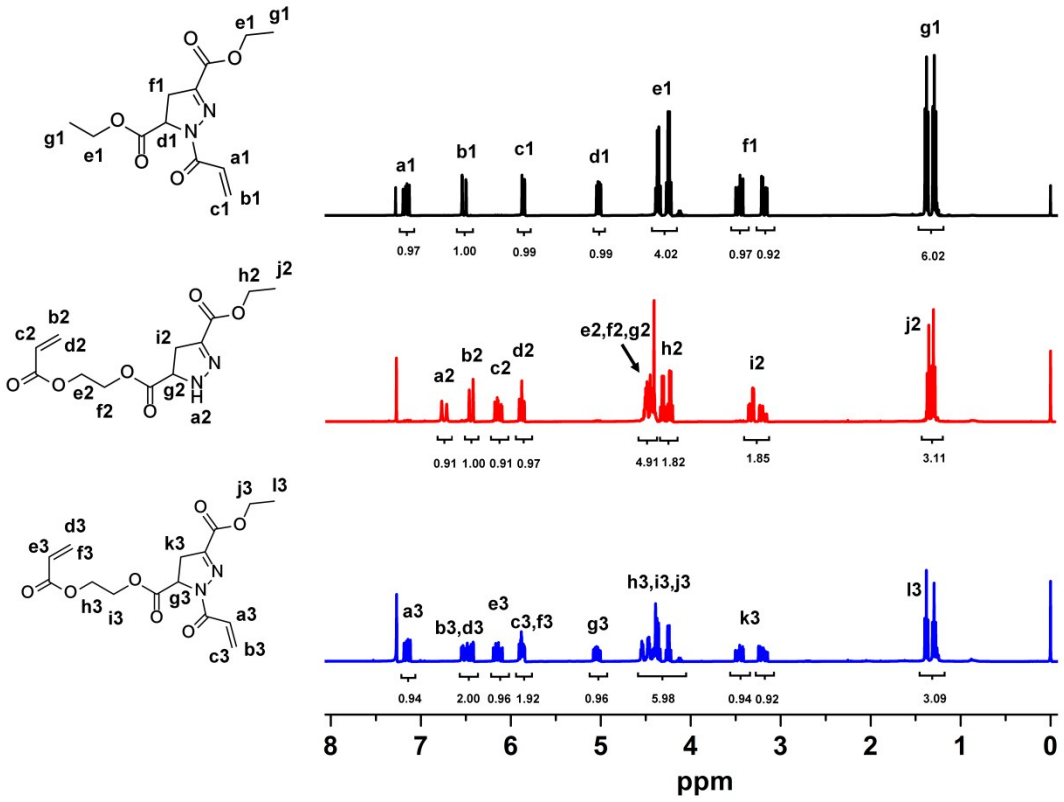

Figure S6 The ^{1}H NMR spectrum of PDP (black line), CACP (red line) and PCAP (blue line).

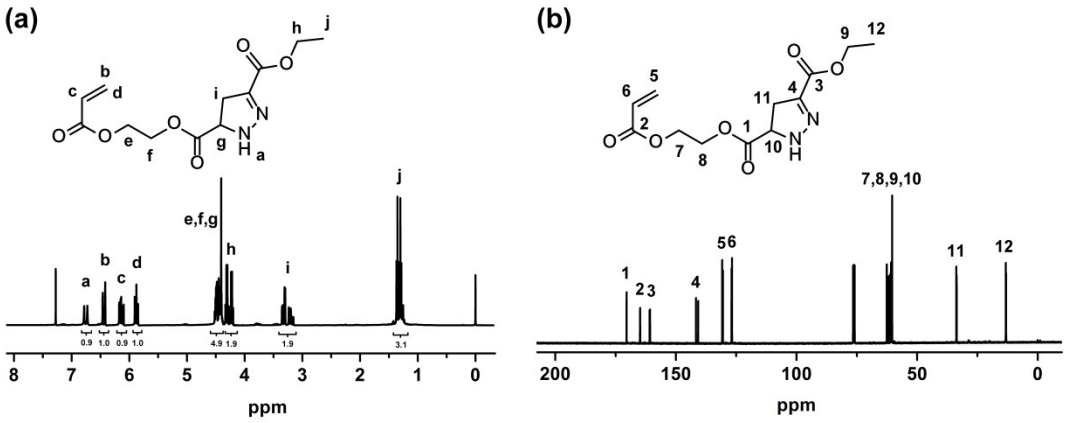

Figure S7 Characterization of the CACP. (a) The ^{1}H NMR spectra of CACP. (b) The ^{13}C NMR spectra of CACP.

Data analysis of the polymerization of CACP. The general synthesis process is illustrated by Scheme S3. AIBN and BPO were used to catalyze the polymerization of CACP (Table S1). The M_n values of most of the polymerization products ranged from 2189 to 7595 g mol^{-1}, which ensured that the polymerization products were oligomers (OCACPs). In the polymerization process, when the ratio value of the monomer to the catalyst was low (runs 1-3), the M_n values were greater, but the product yield sharply declined. Additionally, the quantum yield had a tendency to decrease as the M_n values increased (runs 1-6). In addition, CACP can be

copolymerized with other monomers (run 7-10) with a reactive double bond, and the DSC measurements (Figure S8) for OCACPs indicated that the copolymerization occurred. The nitrogen content of OCACPs ranged from 3.46 to 9.32%, as determined by elemental analysis, and the theoretical values in elemental analysis for OCACP (run 1): C (50.70%), H (5.63%), N (9.86%). In addition, OCACPs exhibited a reverse glass-transition temperature (Figure S8) between 0.6 and 61.8 °C.

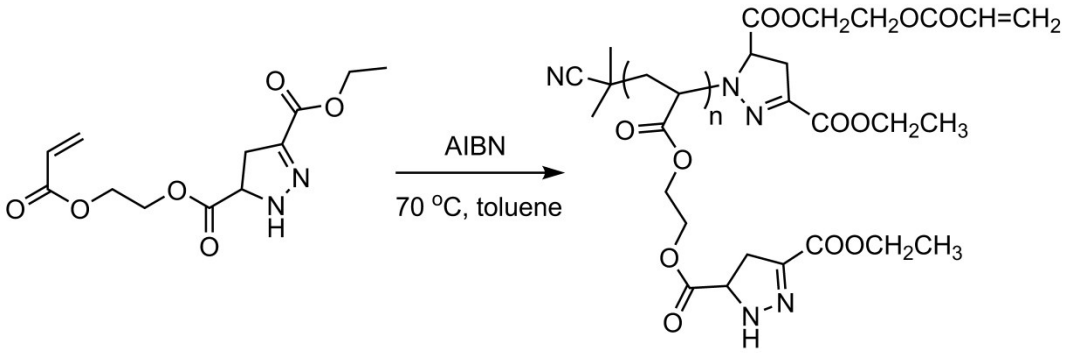

Scheme S3 The synthesis process of OCACPs.

Table S1 The polymerization of CACP[a].

Run	Catalyst	Additive	[M]:[A]:[Cat.] [b]	Yield[c] (%)	M_n[d] (g mol^{-1})	DP[e]	PDI[d]	Elemental analysis (%)			Quantum yield[f] (%)
								C	H	N	
1	AIBN	-	5:0:1	16.4	2189	7.5	1.31	50.82	5.72	9.32	34.23
2	AIBN	-	10:0:1	5.3	2506	8.6	1.35	-	-	-	20.10
3	AIBN	-	20:0:1	1.2	2702	9.3	1.53	-	-	-	10.66
4[g]	BPO	-	5:0:1	13.6	2536	8.7	1.29	52.33	5.05	9.12	41.08
5[g]	BPO	-	10:0:1	4.5	3133	10.8	1.53	-	-	-	28.22
6[g]	BPO	-	20:0:1	1.1	7595	26.5	1.71	-	-	-	11.14
7	AIBN	PMEA	5:5:1	51.2	3596	-	1.58	52.06	6.43	3.46	17.82
8	AIBN	NIPAAm	5:5:1	46.8	4247	-	1.78	52.31	6.18	9.05	9.74
9	AIBN	St	5:5:1	49.7	2912	-	1.49	60.87	5.63	6.12	19.12
10	AIBN	EA	5:5:1	38.7	2193	-	1.26	52.45	5.68	7.53	34.27

[a] At 70 °C for 36 h under nitrogen protection. [b] [M]:[A]:[Cat.] - The molar ratio of the monomer, additive and catalyst. [c] Yield=(the weight of OCACP after re-precipitation three times)/(the weight of the monomer) × 100%. [d] M_n, M_w, and PDI (M_w/M_n) were obtained by GPC with a calibration using standard polystyrenes in THF. [e] DP is the degree of polymerization for each M_n. [f] The quantum yield (QY) was measured using quinine sulfate as the standard (0.1 M H_2SO_4 at 22 °C, QY=58% with excitation at 350 nm) and the Williams and Winfield method. [g] At 80 °C for 36 h under nitrogen protection. PMEA is poly(ethylene glycol) methyl ether acrylate (average M_n of 480), NIPAAm is N-isopropylacrylamide, St is styrene and EA is ethyl acrylate.

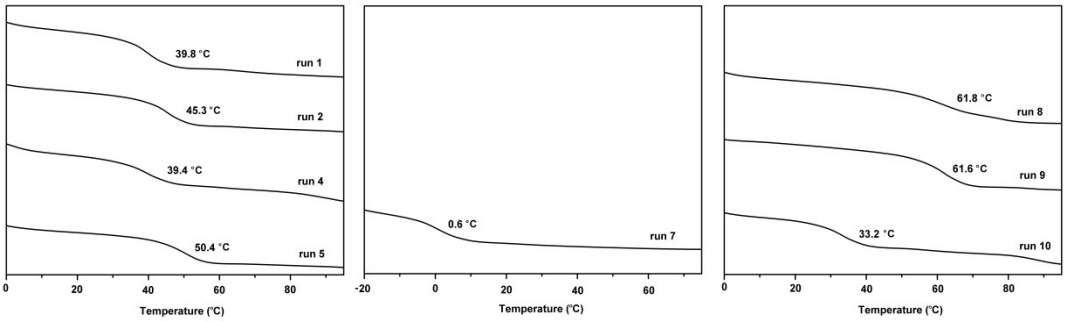

Figure S8 DSC curves of OCACPs (runs 1, 2, 4, 5, 7, 8, 9 and 10).

Characterization of the resulting OCACPs. The ^{1}H NMR spectrum of OCACP (run 1) is shown in Figure S9a. The signals near δ 7.68-7.06 ppm are assigned to -NH-, and the signals near δ 6.53-5.82 ppm are attributed to -CH=CH_2. The signals near δ 4.85-3.99 ppm are ascribed to -OCH_2- and -CH<. The signals near δ 3.38-3.07 are attributed to the methylene (CH_2) group of the pyrazoline ring, and the signals near δ 2.75-1.46 are attributed to -$(CH_2$-$CH)_n$- in the oligomer. The signals near δ 1.44-1.01 are assigned to the methyl group. The ^{13}C NMR spectrum of OCACP (run 1) is shown in Figure S9b. The peaks near δ 14.21 ppm indicate the methyl group (CH_3), and the peaks near δ 27.63 ppm are attributed to the methylene (CH_2) group of the backbone. The peaks near δ 34.37 ppm are attributed to the methylene (CH_2) group of the pyrazoline ring and methyne group (CH) of the backbone. The peaks near δ 64.77-60.75 ppm are attributed to the methylene groups (OCH_2) and methyne group (CH) that are connected to the nitrogen atom. The peaks near δ 134.51-128.37 indicate the double bond and C=N.[5] The peaks at δ 174.60, 172.02 and 160.38 ppm assigned to the carbonyl group. Additionally, OCACPs (runs 7-10) were characterized by ^{1}H NMR spectra (Figure S10-S13).

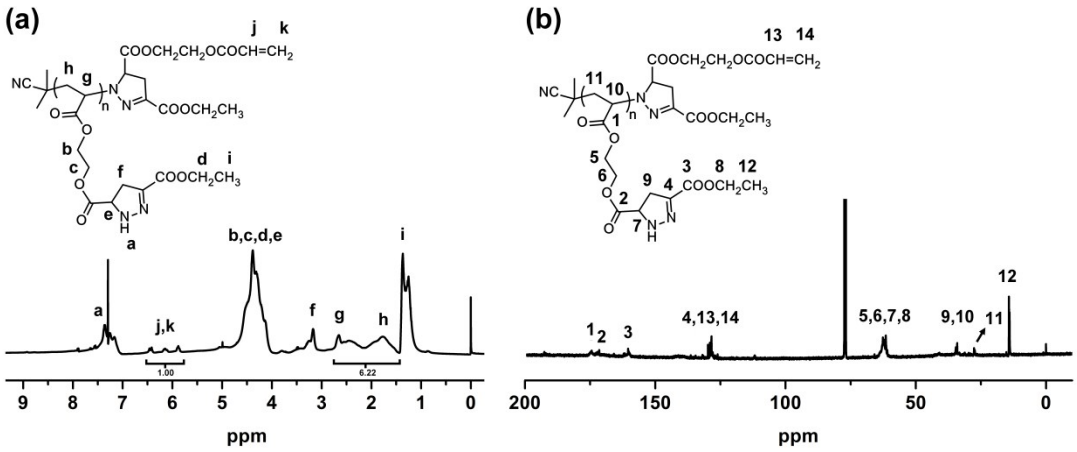

Figure S9 Characterization of OCACP (run 1). (a) The ^{1}H NMR spectra of OCACP (run 1). (b) The ^{13}C NMR spectra of OCACP (run 1).

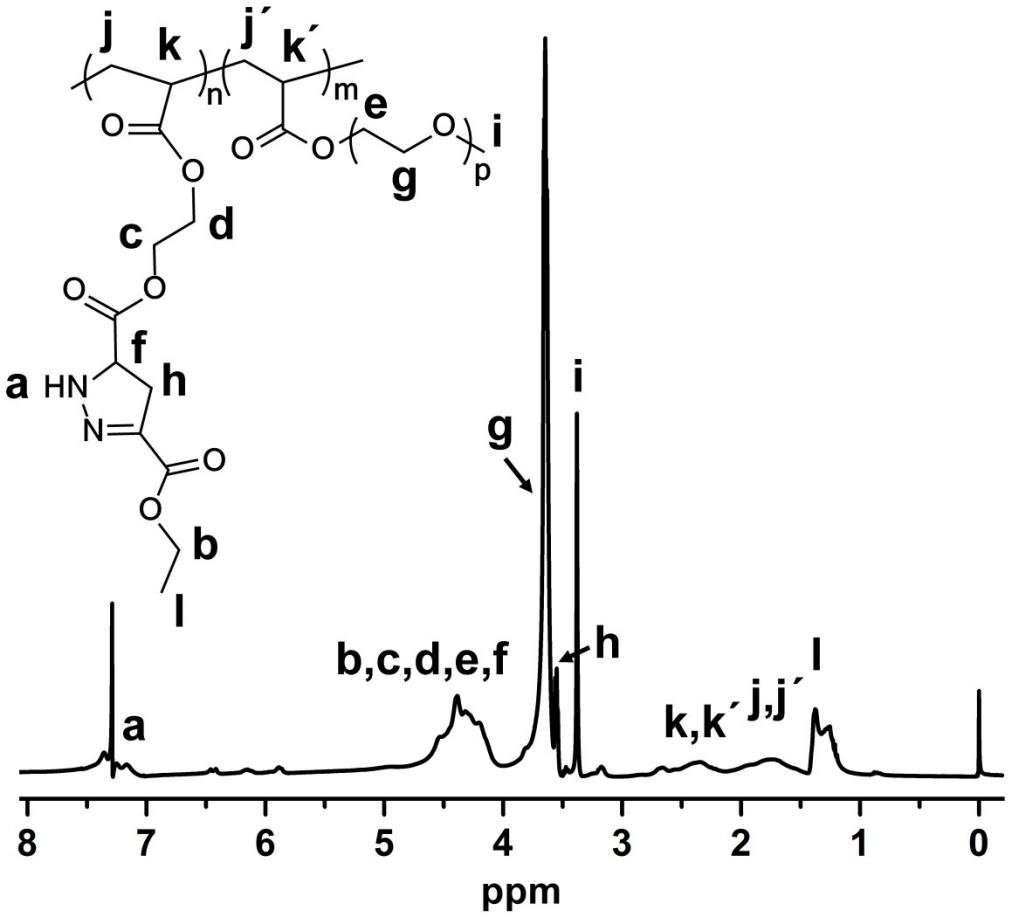

Figure S10 The ^{1}H NMR spectrum of OCACP (run 7).

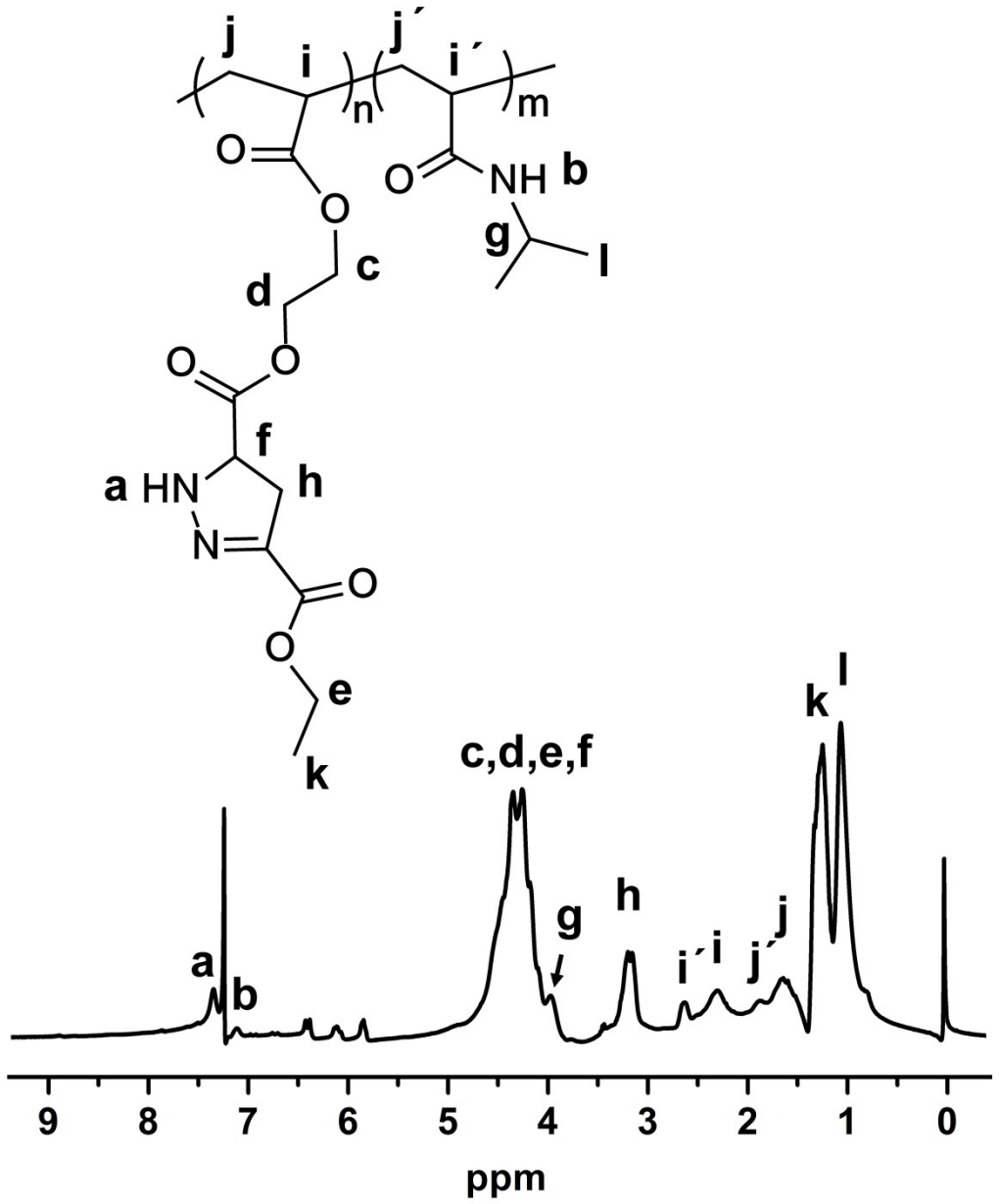

Figure S11 The ^{1}H NMR spectrum of OCACP (run 8).

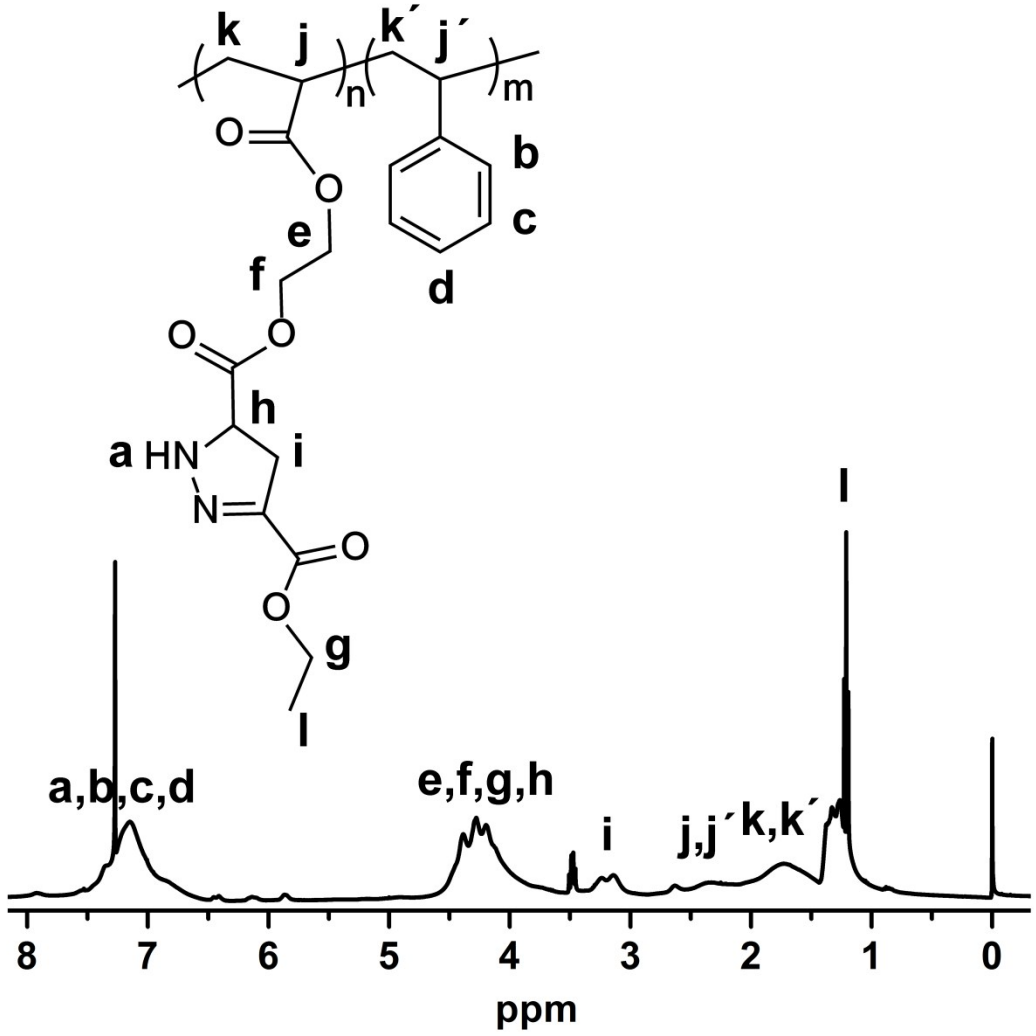

Figure S12 The ^{1}H NMR spectrum of OCACP (run 9).

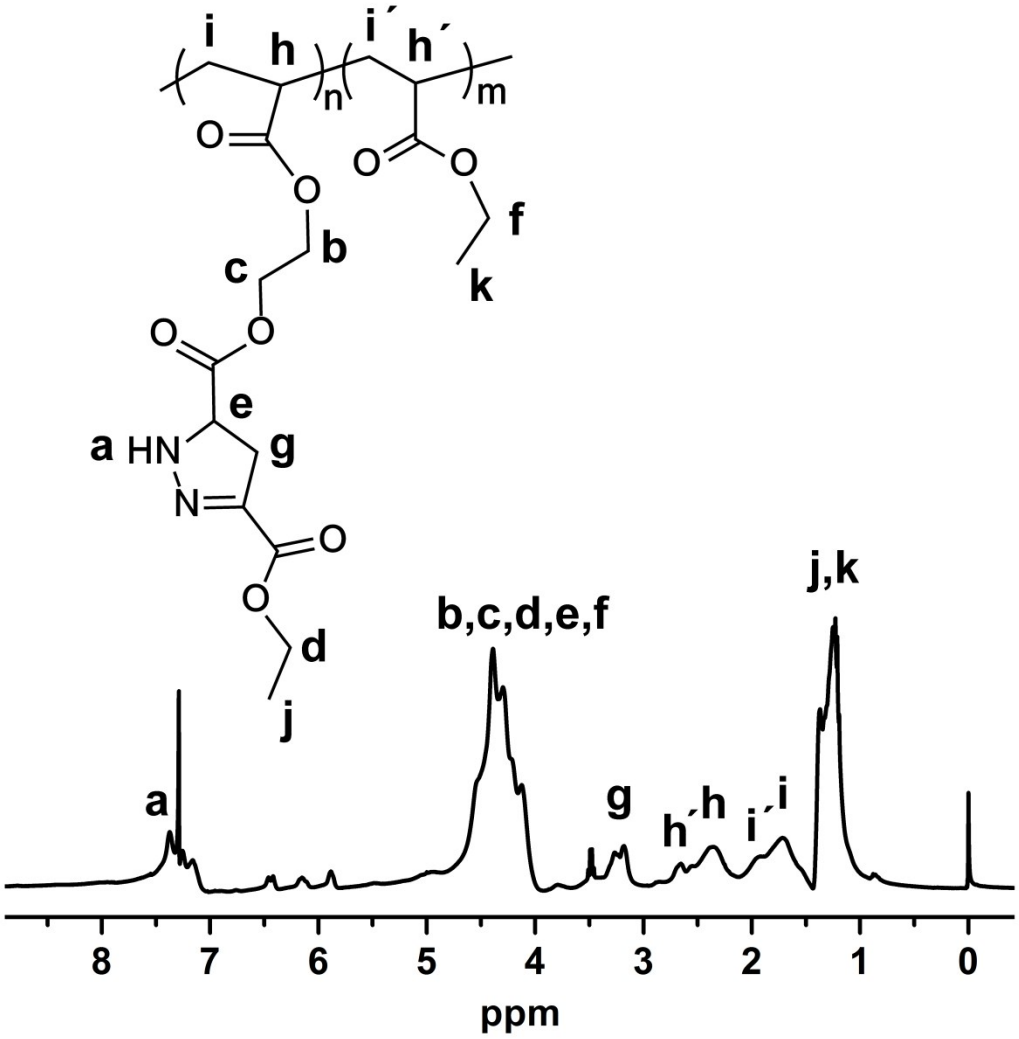

Figure S13 The ^{1}H NMR spectrum of OCACP (run 10).

MALDI-TOF-MS analysis. Figure S14 shows the MALDI-TOF mass spectrum of OCACP (run 1) for m/z values from 1000 to 2500. The primary peaks in the spectrum can be sorted in the following series: Na^{+} + 68 + 283 + 284n (n = 3-6). The main repeating m/z difference in the spectrum of the polymerized product from the AIBN-catalyzed reaction (run 1) is the peak at m/z 284 (Figure S14, series A1 to A4), which is the mass of CACP. Additionally, the mass of dehydrogenated CACP is 283, and the deviation in the calculated segment mass from the measured m/z for series A is 68, which is half the mass of denitrogenated AIBN. Based on the MALDI-TOF-MS results, we propose the reaction mechanism shown in Figure S15. In the initiation step, $CN(CH_3)_2CH\cdot$ is formed by thermal decomposition of AIBN. In the propagation step, the double bond of CACP is initiated by $CN(CH_3)_2CH\cdot$, and the polymer backbone is propagated by a free-radical transfer. In addition, the N-H bond of CACP undergoes cleavage via the reactive hydrogen combining with $CN(CH_3)_2CH\cdot$. In the termination step, the polymer backbone ends with the deprotonation of CACP. In addition, the molar ratio (MR) of $-CH_2-CH-$ and $CH_2=CH-$ in OCACP (run 1) can be determined from the M_n value and integral area ratio of the corresponding region in the NMR spectrum. The M_n value of OCACP (run 1) is 2189, and after subtracting the terminal

group molecular weight, the MR is 6.47, which agrees well with the NMR integral area ratio value of 6.22 (Figure S9). The two calculated results indicate that the proposed mechanism is reasonable.

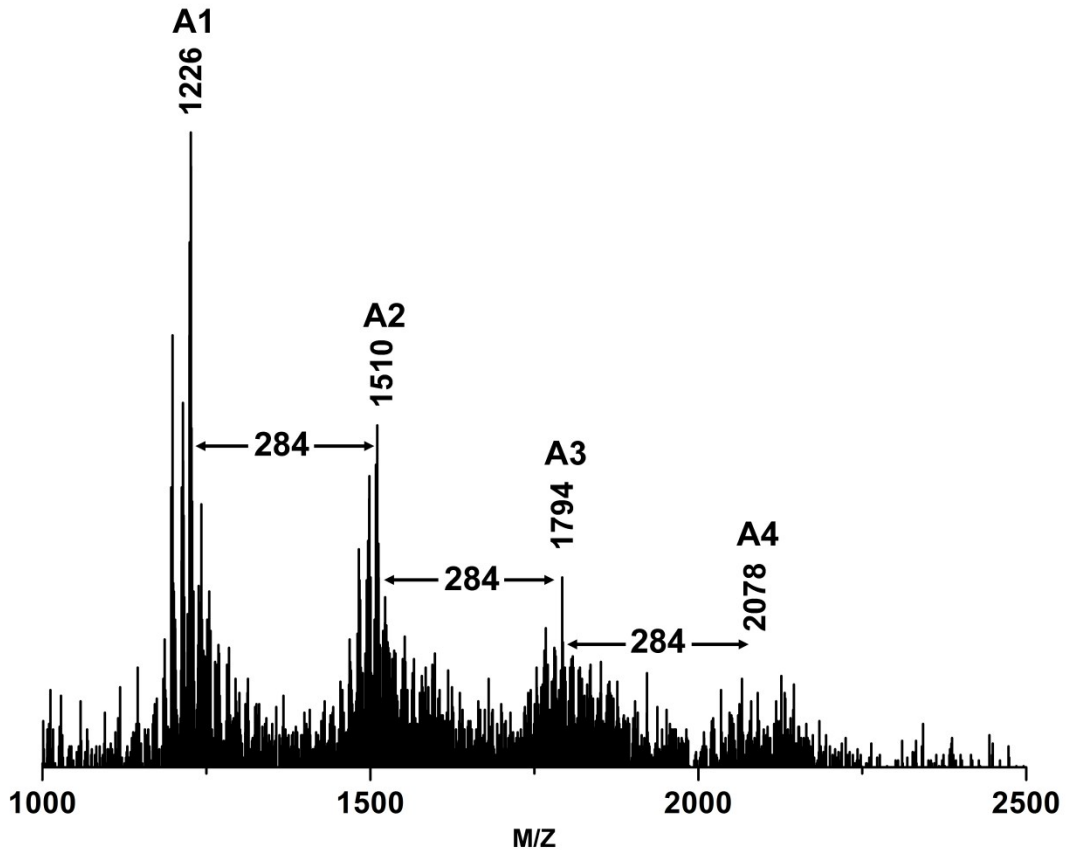

Figure S14 The MALDI-TOF mass spectrum of OCACP (run 1).

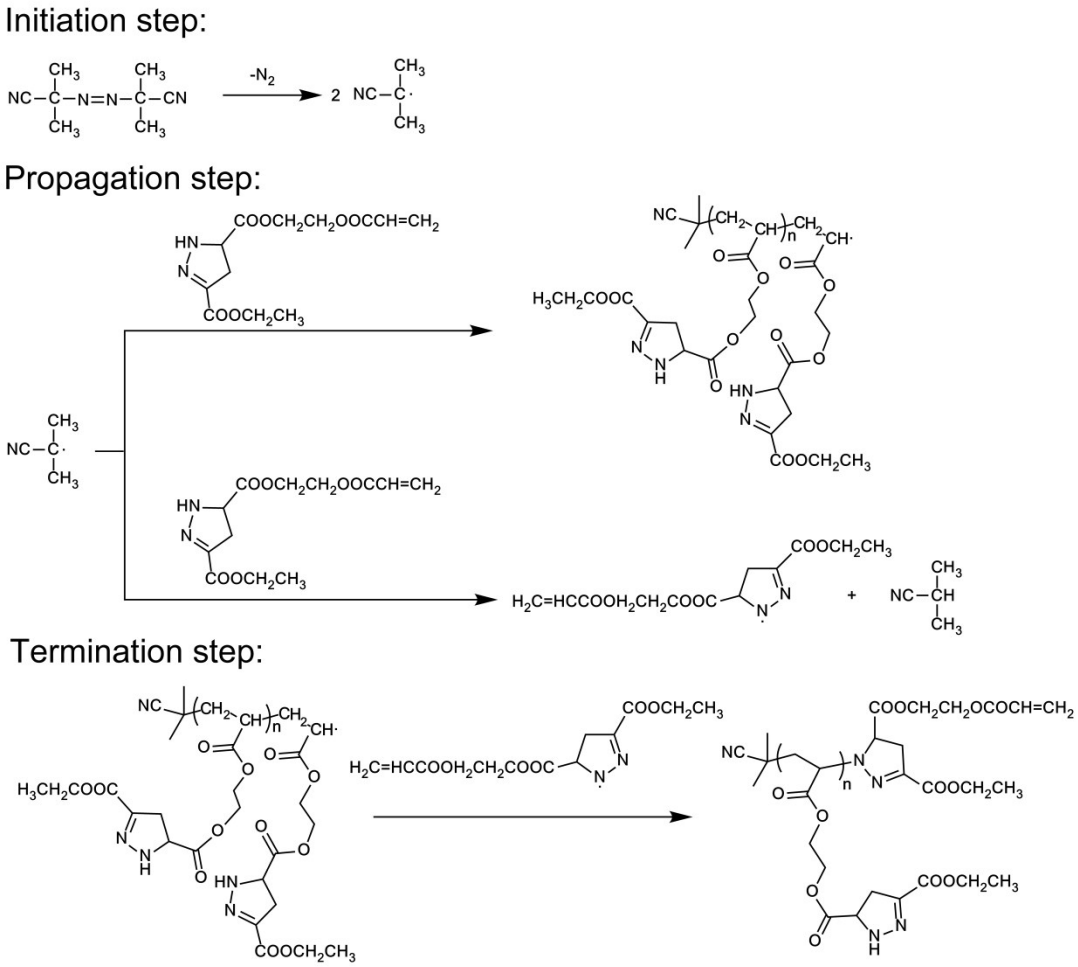

Figure S15 The proposed oligomerization mechanism catalyzed by AIBN.

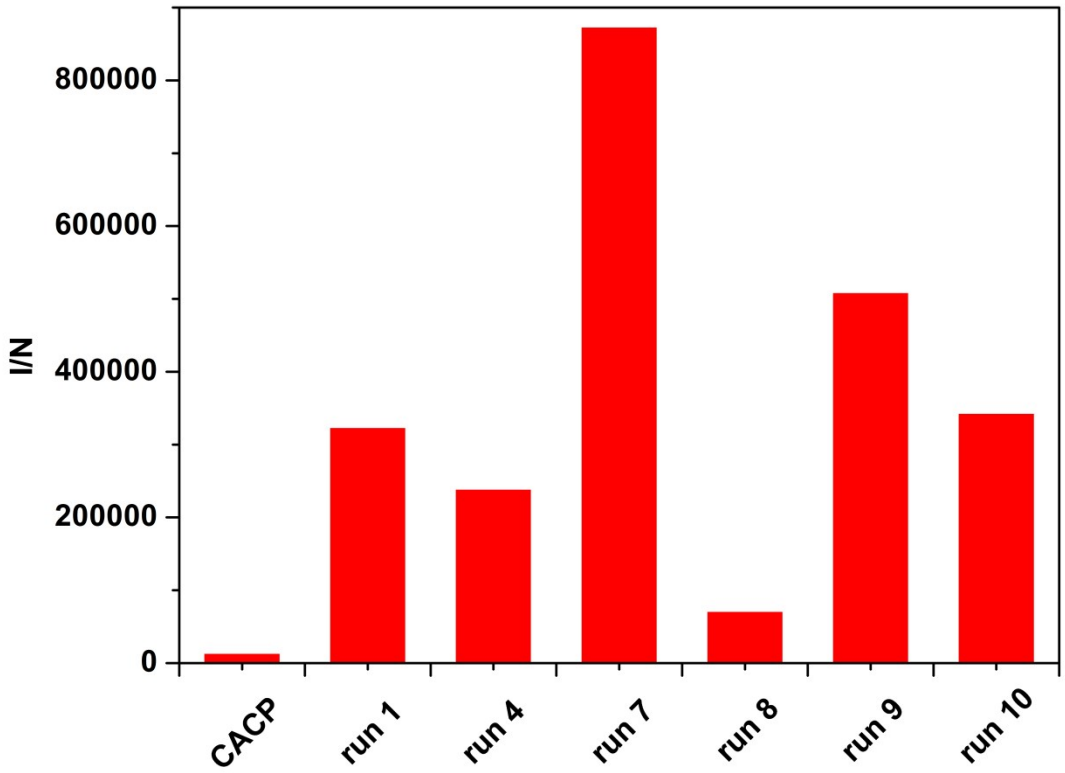

Figure S16 I/N of 0.03 mg mL^{-1} of CACP and OCACPs (runs 1, 4, 7, 8, 9 and 10) in chloroform. I: the maximum fluorescence emission intensity; N: the concentration of nitrogen atoms, where N = (the content of nitrogen obtained by elemental analysis) × (the concentration of the solution); I/N: the maximum fluorescence emission intensity for a nitrogen atom of 1 mg mL^{-1}, named as the molecular fluorescence emission efficiency.

Table S2 The visible light region integrated intensity (425-592 nm) of chloroform and OCACP (run 1) under different power irradiation of a 300 W Xe lamp (PLS-SXE 300, Beijing Perfectlight Co. Ltd) without filter.

I (A)[a]	Chloroform [b]	OCACP [c]
14	34297	36542
15	40241	46310
16	49957	54708
17	56845	64699
18	65936	74578
19	75147	86809
20	83374	98412

[a] I represents the magnitude of current of a 300 W Xe lamp (PLS-SXE 300, Beijing Perfectlight Co. Ltd). [b] Chloroform represents the visible light region integrated intensity (425-592 nm) of chloroform under different power irradiation of a 300 W Xe lamp (PLS-SXE 300, Beijing Perfectlight Co. Ltd) without filter. [c] OCACP represents the visible light region integrated intensity (425-592 nm) of OCACP (run 1) under

different power irradiation of a 300 W Xe lamp (PLS-SXE 300, Beijing Perfectlight Co. Ltd) without filter.

Table S3 The relationship between the intensity of incident light of RF-5301PC (Shimadzu) fluorescence spectrophotometer and photoluminescence integrated intensity (PLII).

Incident SW[a]	Reception SW[a]	Additive[b]	I_{688}[c] (μA)	$I_{346+688}$[c] (μA)	P_{346}[c] (μW cm^{-2})	PLII[d] (a.u.)
20	3	-	1.27	5.27	801	87989
20	3	Glass slide	1.10	4.90	711	67802
15	3	-	0.80	4.20	616	49001
15	3	Glass slide	0.63	3.73	540	37640
10	3	-	0.43	3.00	418	26287
10	3	Glass slide	0.30	2.53	362	19136

[a] Incident SW is incident light slit width and Reception SW is reception light slit width. [b] The glass slide was placed closely to the position with incident light emission to appropriately reduce the intensity of incident light. [c] I_{688} is the optical induction current value of 686 nm part of incident dichromatic light measured by solar panel in the sample cell, $I_{346+688}$ is the optical induction current value of incident dichromatic light measured by solar panel in the sample cell, P_{346} is the optical induction power of 346 nm part of the incident dichromatic light measured by UVA light meter in the sample cell. [d] PLII is the photoluminescence integrated intensity of 368-635 nm region.

Table S4 The relationship between the intensity of incident light of supfire UV03-365 flashlight and the corresponding photoluminescence integrated intensity (PLII).

Reception SW[a]	P_{365}[b] (mW cm^{-2})	PLII[c] (a.u.)
5	5.63	68624
5	4.82	61066
5	4.14	53656
5	3.62	47094
5	3.21	40614
5	2.78	35698

[a] Reception SW is reception light slit width. [b] P_{365} is the optical induction power of 365 nm light of supfire UV03-365 flashlight measured by UVA light meter in the sample cell. [c] PLII is the photoluminescence integrated intensity of 407-650 nm region.

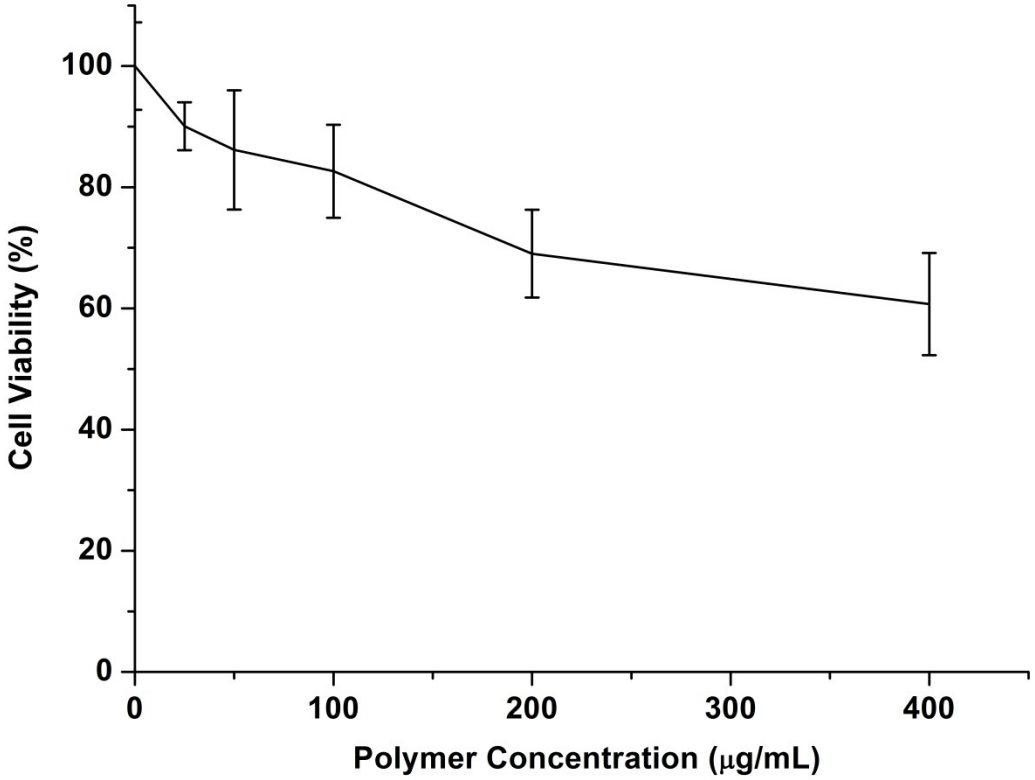

Figure S17 Cytotoxicity of the oligomer (run 1) in Hela cells.

Cytotoxicity Assay. Cell viability was determined by using a standard 3-(4,5-dimethyl- 2-thiazolyl)-2,5-diphenyl-2-H-tetrazolium bromide (MTT) assay. HeLa cells were seeded in 96-well plates at a concentration of 5×10^3 cells/well in a final volume of 200 μL and incubated for 24 h. The cells were then incubated with OCACP (run 1) dissolved in complete cell culture medium at final concentrations of 0, 25, 50, 100, 200 and 400 μg/mL. After 48 h incubation, 20 μL of MTT (5 mg/mL, Sigma) solution was added to each well and incubated for 4 h at 37 °C with 5% CO_2. The supernatant was then removed, and the cells treated with 200 μL of dimethyl sulfoxide (DMSO, Sinopharm, China), followed by gently shaking. The plates were analyzed at a wavelength of 570 nm on a microplate reader (TECAN, SPARK 10M, Austria). The data was presented as cell viability (%) = Experimental group/Negative control group × 100%.

References

1. J. D. Clark, J. D. Heise, A. S. Shah, J. C. Peterson, S. K. Chou, J. Levine, A. M. Karakas, Y. Ma, K.-Y. Ng and L. Patelis, Org. Process Res. Dev., 2004, 8, 176-185.
2. G. Li and C. Che, Org. Lett., 2004, 6, 1621-1623.
3. C. Chen, Y. Li, X. Jia, F. Li, F. Chen, L. Liu, *New Journal of Chemistry*, 2017, **41**, 3719-3722.
4. X. Jia, Y. Li, L. Xiao and L. Liu, *Polym. Chem.*, 2014, **5**, 4781-4789.
5. S. B. Zangade, S. S. Mokle, A. T. Shinde and Y. B. Vibhute, Green Chem. Lett. Rev., 2013, 6, 123-127.